HAL
open science

A phenomenological model of starch expansion by extrusion

Magdalena Kristiawan, Guy G. Della Valle, Kamal Kansou, Amadou Ndiaye, Bruno Vergnes, Combe David

To cite this version:

Magdalena Kristiawan, Guy G. Della Valle, Kamal Kansou, Amadou Ndiaye, Bruno Vergnes, et al.. A phenomenological model of starch expansion by extrusion. Rhéologie, 2015, 27, pp.24-33. hal-01410168

HAL Id: hal-01410168

https://minesparis-psl.hal.science/hal-01410168v1

Submitted on 6 Dec 2016

HAL is a multi-disciplinary open access archive for the deposit and dissemination of scientific research documents, whether they are published or not. The documents may come from teaching and research institutions in France or abroad, or from public or private research centers.

L'archive ouverte pluridisciplinaire **HAL**, est destinée au dépôt et à la diffusion de documents scientifiques de niveau recherche, publiés ou non, émanant des établissements d'enseignement et de recherche français ou étrangers, des laboratoires publics ou privés.

A phenomenological model of starch expansion by extrusion

M. Kristiawan[1], G. Della Valle[1], K. Kansou[1], A. Ndiaye[2], B. Vergnes[3] and C. David[4]

[1] *INRA, UR 1268 Biopolymers Interactions and Assemblies (BIA), BP 71627, 44316 Nantes*

[2] *INRA, USC 1368 Institut de Mécanique et d'Ingénierie (I2M), UMR 5295 CNRS, Université Bordeaux 1, 33405 Talence Cedex*

[3] *MINES ParisTech, CEMEF, UMR CNRS 7635, BP 207, 06904 Sophia-Antipolis Cedex*

[4] *Sciences Computers Consultants, 10 rue du Plateau des Glières 42000 Saint-Etienne*

Reçu le 16 décembre 2014 - Version finale acceptée le 17 novembre 2014

Abstract: During extrusion of starchy products, the molten material is forced through a die so that the instantaneous pressure drop causes part of the water to vaporize, giving an expanded, cellular structure. The objective of this work was to elaborate a phenomenological model of expansion and couple it with Ludovic® mechanistic model of twin screw extrusion process. From experimental results that cover a wide range of thermomechanical conditions, a concept map of influence (relationships between input and output variables) was built. It took into account the phenomena of bubbles nucleation, growth, coalescence, shrinkage and setting, in a viscoelastic medium. The input variables were the moisture content *MC;* melt temperature T_p, specific mechanical energy *SME*, shear viscosity η at the die exit, computed by Ludovic®, and the melt storage moduli E'(at $T_p > T_g$). The outputs of the model were the macrostructure (volumetric expansion index *VEI*, anisotropy) and cellular structure (fineness) of solid foams. Then a general model for *VEI* was suggested and the link between anisotropy and fineness was established.

Keywords: starch, extrusion, anisotropy, cellular structure, elongational viscosity, shear viscosity

[Abridged French version on last page]

1. Introduction

Extrusion is extensively used for production of different categories of starch based foods. After melting, the viscous material is forced through a die where a part of superheated water evaporates due to the instantaneous pressure drop. The vapor blows the material to an expanded, porous structure. The product cools down due to the evaporation and convective heat transfer and, crossing the glass transition, it becomes solid. The expansion at the die exit is thus a very complex process involving a succession of dynamic phenomena, occurring in a short time interval (less than 1 s), such as bubble nucleation and growth, coalescence, shrinkage and finally setting when the melt matrix becomes glassy. Hence, extruded products can have same density but different cellular architectures depending on the raw material formulation and processing parameters [1, 2]. Both features in-turn impact the texture, nutritional and sensory attributes of the product.

The growth of a bubble was modelled mechanically using a “cell model” [3] in which the gas bubble is surrounded by an envelope of liquid (with finite thickness), providing a finite amount of liquid for expansion and thus limiting the final radius of the bubble. The expansion rate depends on the pressure difference across the shell of bubbles and on the rheological properties of starch melt (shear viscosity). This model presents two important features: depletion of dissolved gas and progressively thinning bubble walls. Thereafter, other models followed a similar approach and the main differences between them can be classified according to the assumptions made [4-11]: presence of heat transfer, dependence of physical parameters (shear viscosity, diffusion coefficient) on temperature and moisture content, coupling microscopic bubble growth model (on bubble scale) with macroscopic mass, momentum and heat transfer (on the extrudate scale) and rheological model for the melt. Different forms of the equation of motion linking the bubble radius with the pressure in the bubble can be distinguished, by taking into account or not the surface tension effects, elastic effects, yield stress and inertial terms.

Most authors modelled the expansion as the sequence of bubble growth and shrinkage phenomena only and did not take into account the nucleation and coalescence. They also often took an initial bubble number as parameter, and all neglected the role of elongational viscosity. Pai et al. [12] suggested that the extrudate expansion depends on the interplay of shear and extensional viscosities. These various numerical mechanistic models are thus not complete, but they are also too complex to be coupled with present software for simulation of co-rotating twin-screw extrusion process (Ludovic®) [13]; so there is a need for simpler model in order to extend the capability of this software to predict the cellular structure of starchy extruded foams.

The objective of this work was to elaborate a phenomenological model of expansion in function of processing variables and melt rheology, and thereafter to couple it with Ludovic® mechanistic model. Qualitative representation, using concept map, was used to reason about the physical process of vapor expansion, in order to improve our understanding and to suggest a mathematical expression of the phenomenological models. The melt rheology involved shear and elongational viscosities. The input variables such as melt temperature T_p, specific mechanical energy *SME* and shear viscosity η can be computed by Ludovic®. The other inputs were moisture content *MC* and die geometry. The output variables were the foam macrostructure, described by anisotropy (*AF*) and bulk expansion indices (*VEI* and *SEI*) deduced from density, and cellular microstructure assessed by fineness (*F*), computed from mean cell size and mean cell wall thickness.

2. Materials and methods

2.1. Materials and extrusion conditions

The modeling work was realized on the published data of maize starches expansion using a twin-screw extruder (Clextral BC45) equipped with a slit die rheometer (Rheopac) [1, 14-16]. For each experiment, die temperature, product temperature at die exit, intensity of main motor drive and thrust bearing pressure were measured. The latter was measured using stress gauge. Specific mechanical energy (*SME*) was calculated from the screw speed, mass flow rate and measured intensity [17]. Maize starches with different amylose content were used to study the influence of elongational viscosity (Table 1). The overview of extrusion variables is shown in Table 2. As a general rule, low moisture content led to medium or high *SME* and T_p whereas high moisture content gave low or medium *SME* and T_p.

Starch	Product	Amylose / Amylopectin
A	Amylomaize	70 / 30
B	Blend A : D = 2 : 1	47 / 53
C	Blend A : D = 1 : 2	23.5 / 76.5
D	Waxy maize	0 / 99

Table 1. Raw material

Extruder configurations and sets of operating conditions have been fully detailed formerly [14]. For each experimental set (combination of amylose content, *MC*, T_p, *SME*, die height), the shear rate in the Rheopac channels was varied between 10 and 200 s^{-1}, and the melt shear viscosity has been determined from pressure drop in measuring channel, after Rabinowitsch corrections. The measuring channel was provided with three pressure sensors (Dynisco, 0-10 MPa), each spaced by 5 cm, the last one at 3 cm from the die outlet. The extruded ribbon was collected from measuring channel for structural characterization after drying and conditioning to a moisture content of about 0.1 (mass fraction on dry basis).

Control variables	*MC*[1]	T_p (°C)	*SME* (kWh.t^{-1})	η Pa.s	Die height[2] h_d (mm)	Entrance opening[3] h (mm)
Min	0.21	105	101	80	3	0.3
Max	0.36	186	580	1200	2	3

[1]mass fraction on total wet basis
[2]Rheopac main channel height
[3]Orifice opening of the entrance of the measuring channel

Table 2. Operating variables at the die exit

2.2 Structural characterization

2.2.1 Macrostructure

The bulk expansion indices, *VEI* for volumetric, *SEI* for radial and *LEI* for longitudinal expansion, were defined according to the definitions given by Alvarez-Martinez et al. [18]. Longitudinal means the expansion is in the die flow direction and radial in the orthogonal plane.

$$VEI = \frac{\rho_m\left(1-MC_m\right)}{\rho_e\left(1-MC_e\right)} \quad (1)$$

$$SEI = \frac{S_e}{S_d} \quad (2)$$

$$LEI = S_d\, L_{se}\, \rho_m \frac{1-MC_m}{1-MC_e} \quad (3)$$

where ρ is the density (kg.m^{-3}), *MC* is the moisture content (mass fraction on total wet basis), *S* is the cross section (m^2) and L_{se} is the specific length of extrudate (m.kg^{-1}). Subscripts *d*, *e* and *m* refer to die, extrudate and melt, respectively. The extrudate bulk

density ρ_e was measured by beads displacement. L_{se} was measured with a Vernier caliper.

Finally, *VEI* can be defined as

$$VEI = LEI \times SEI \quad (4)$$

On the basis of observations made by Arhaliass et al. [19] and Robin et al. [2], considering that *SEI* involves two spatial dimensions and *LEI* one, it can be assumed that for isotropic expansion: $LEI = SEI^{0.5}$. The anisotropy factor (*AF*) was thus defined as:

$$AF = \frac{LEI}{SEI^{0.5}} = \frac{VEI}{SEI^{3/2}} \quad (5)$$

If *AF* is greater than 1, the longitudinal expansion prevails the radial expansion and vice versa.

As *LEI* was found to have the largest measurement error (20%) compared to *VEI* (10%) and *SEI* (8%) [15], the use of *VEI* and *SE*I as macrostructure model outputs is more convenient.

2.2.2 Cellular structure

The mean cell size (*MCS*) and mean cell wall thickness (*MWT*) of extruded starch foams were determined from the volumetric distributions of cells and cell walls after analyses of 3D images acquired by X-ray tomography by Babin et al. [1]. Then we defined the fineness (*F*) of the microstructure by:

$$F = \sqrt{\frac{\left(\frac{MCS_{av}}{MCS}\right)^2 + \left(\frac{MWT_{av}}{MWT}\right)^2}{2}} \quad (6)$$

where MCS_{av} and MWT_{av} are average values for *MCS* and *MWT*, equal to 1 mm and 250 µm, respectively [1, 2]. Then $F > 1$ means extrudate has a fine cellular structure and $F < 1$ a coarse one.

2.3. Modelling approach

Because of the complexity of expansion phenomena, the first stage involved the knowledge reasoning approach: (a) collecting scientific knowledge from literature, expertise and experimental data, (b) representing knowledge with concept map. Using the concept map (influence graph), the direction and magnitude of influence relationships between input variables and expansion phenomena and output variables were determined. Then the net effect of input variables on one output variable was deduced.

In the second stage, the phenomenological models for volumetric (*VEI*) and radial (*SEI*) expansion indices were established using variables defined in the previous step and literature data [1, 14, 15]. The anisotropy factor (*AF*) was computed from *VEI* and *SEI* models and compared to experimental data, using Eq. 5. The cell fineness (*F*) was finally related to *AF*.

The validity of Ludovic® simulation results for flow variables in an extruder was also verified. For the molten maize starches (with amylose content of 0 and 0.23), the constants (*K* and *n*) of power law model for shear viscosity η were expressed according to [14]:

$$\eta = K\dot{\gamma}^{m-1} \quad (7)$$

$$K = K_0 \exp\left(\frac{E}{RT} - \alpha MC - \beta SME\right) \quad (8)$$

$$m = m_0 + \alpha_1 T + \alpha_2 MC + \alpha_3 SME + \alpha_{12} T\,MC + \alpha_{13} T\,SME + \alpha_{23} MC\,SME \quad (9)$$

Detailed information concerning the *SME*-shear viscosity coupling mode can be found elsewhere [20]. The shear viscosity at the die exit was also calculated using Ludovic®.

2.4. Least square fit of model and statistical analysis

Data regression was performed using non-linear least square (NLLS) method by Microsoft Excel Solver. Then the statistical analysis was done using SOLVERSTAT, in Microsoft Excel that yields the statistical regression diagnostics after LS fitting by Solver [21].

The models must pass following checks for regression analysis: (1) Examination of model quality with a *F*-Test. If $F_{calc.} > F_{crit.}$, then the regression is significant. (2) Examination of regression method quality using *Levene F*-Test to check that residuals have constant variance (if $F_{calc.} < F_{crit.}$ is fulfilled). (3) Examination of significativity model parameters with a Student *t*-Test that checks if the single parameter is statistically different from zero (if $t_{cal.} > t_{crit.}$ is fulfilled). (4) Examination of goodness model fit using several statistical criterias: high value of Coefficient of Multiple Determination R^2, Adjusted Coefficient of Multiple Determination $R^2_{adj.}$ and low value of Root Mean Squared Error (*RMSE*). After discarding non-significant model parameters, the NLLS fitting and SOLVERSTAT were re-launched for reduced *VEI* and *SEI* models.

NLLS fit for *VEI* and *SEI* with objective of minimizing the squared errors of the prediction (*SSE*) has first given high R^2 values, 0.93 and 0.85 (results not shown). Then anisotropy factor (*AF*) computed from these *VEI* and *SEI* models, according to Eq. (5), did not fit the experimental data (R^2 = 0.17). Thus, we used an optimization strategy to

obtain similar values for R^2 of *VEI*, *SEI* and *AF* by minimizing the weighted sum of *SSE* of *AF*, *SEI* and *VEI* in NLLS fit:

$$SSE_{opt} = SSE_{AF} + w_1\, SSE_{SEI} + w_2\, SSE_{VEI} \qquad (10)$$

with weights $w_1 = 0.3$ and $w_2 = 0.05$

By the means of the weights w_1 and w_2, we changed the R^2 of *AF*, *SEI* and *VEI* simultaneously.

The weights $w_1 = 0.3$ and $w_2 = 0.05$ were chosen by trial and error method which assured a high value of R^2 for *AF* (0.78) keeping the both R^2 for *SEI* (0.77) and for *VEI* (0.88) high enough, see Tables 3 and 4.

3. Results and discussion

3.1 Qualitative reasoning of vapor expansion

The concept map defined relations between input variables (temperature of product at die exit T_p, moisture content *MC*, shear viscosity $\eta(\dot{\gamma})$, storage modulus *E*', expansion phenomena (nucleation, bubble growth, coalescence, shrinkage, setting) and output variables as foam density (Fig. 1) and anisotropy factor. These relations are qualitative; they are expressed by the signs + or –. The sign + signifies positive effect and the sign – stands for negative effect. The magnitude of the effect is quantified with a number of signs. The net effect of one input variable on one output variable is the sum of all effects between these variables.

At present, the data of elongational viscosity of starchy products is scarce in literature due to technical difficulties in measurements. Conversely, the storage modulus *E*' in the rubbery domain (i.e. at $T > T_g$, T_g being the glass transition temperature), measures the stored energy and represents the elastic behavior of a viscoelastic fluid. We assume thus that this variable could replace the elongational viscosity in the model because it also reflects an elastic property [1, 12] (Fig. 1). Indeed, according to Babin et al. [1], storage modulus in the rubbery state and elongational viscosity of molten maize starches rank in the same way with amylose content. Della Valle et al. [22] confirmed that elongational viscosity of molten starch pellets of different botanical origins increased with increasing amylose content. The ad-

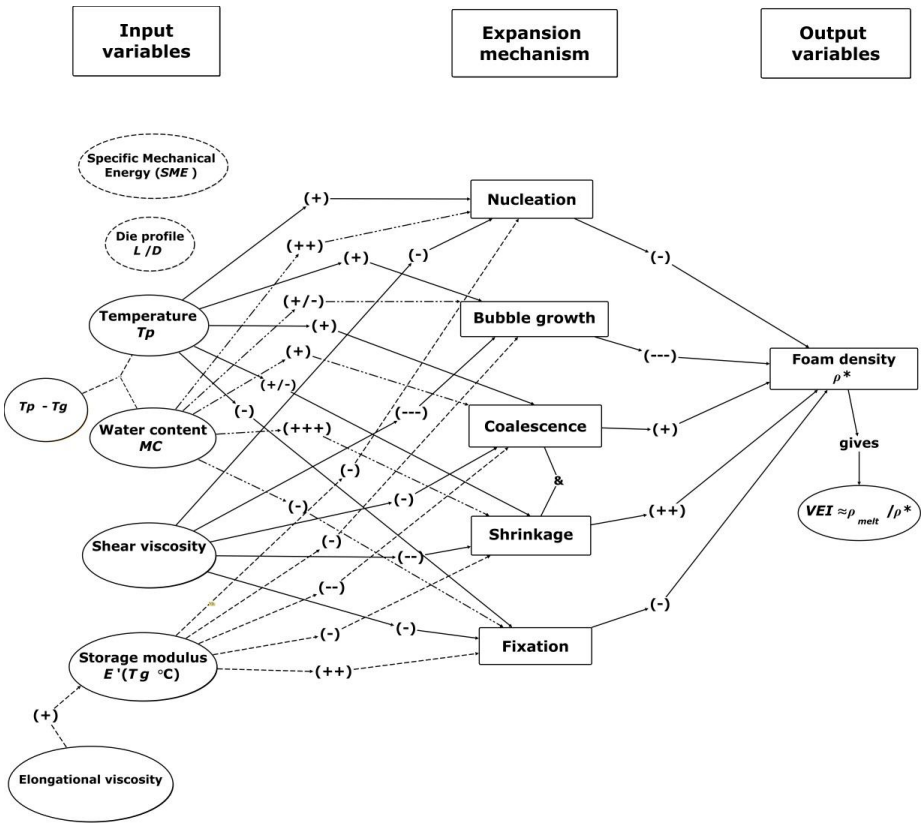

$$\rho^* \approx [MC]^x \otimes [T_p]^y \otimes [E'(T_g)]^z \otimes [\eta(\dot{\gamma})]^t$$

Figure 1. Concept map of phenomenological model of expansion

vantages are that measurements of *E*' are less difficult than those of elongational properties and results are available from literature for various starchy material compositions [1, 23-25].

3.2 Validation of Ludovic® simulations

A good agreement between the computed and measured melt temperature at the die exit was found (data not shown). Although a good correlation between computed and measured *SME* was obtained (R^2 = 0.8 - 0.9), the computed total dissipated energy (total *SME*) was generally underestimated (Fig. 2), likely because Ludovic® model takes into account only the viscous dissipation after melting section and neglects mechanical energy delivered to the product for melting, solid friction and conveying. Conversely, *SME* measured from the torque of the motor takes into account these different phenomena.

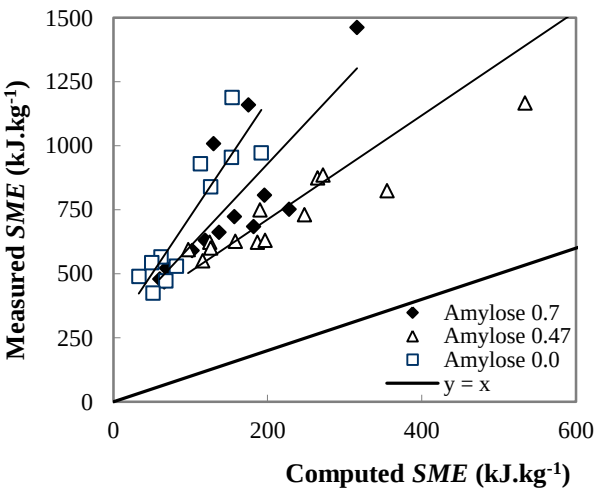

Figure 2. Validation of Ludovic® simulation for *SME*

The computed *SME* was useful to predict starch destructurization during the extrusion process (Fig. 3). The starch destructurization influences the melt shear viscosity [14] and thus the degree of expansion. The starch destructurization was quantified by decrease of material intrinsic viscosity (mL.g^{-1}) after extrusion. The good correlation between starch destructurization (%) and *SME* (R^2 = 0.85 - 0.95) was obtained for starch with amylose contents of 0.47 and 0.0. On the other hand, a poor correlation (R^2 = 0.47) was found for amylose content of 0.7 (Fig. 3). The amylopectine with high molecular weight ($M_w \approx 10^8$ kg.mol^{-1}) was found more sensitive to thermomechanical treatment than amylose of lower molecular weight ($M_w \approx 10^6$ kg.mol^{-1}).

In conclusion, the Ludovic® simulation was reliable to compute the flow variables at the die exit, that can be used, in turn, as the input variables for expansion phenomenological model.

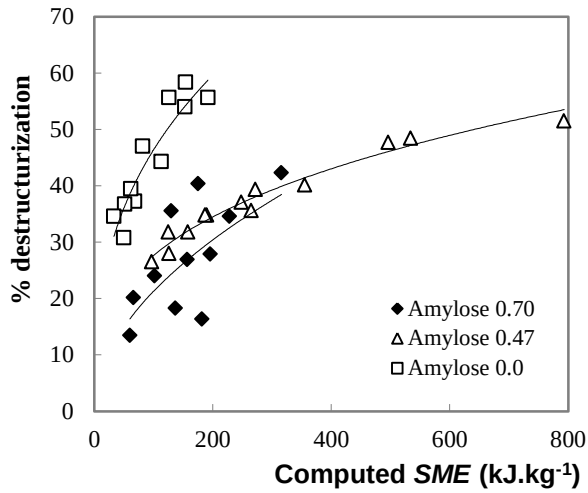

Figure 3. Variations of starch destructurization with *SME*

3.3 Phenomenological model of expansion

As shown by experimental results in Fig. 4, the expansion index *VEI* decreased with shear viscosity following a power-law trend. *VEI* also decreased with increasing moisture content at constant shear viscosity and close to melt temperature [15]. The same tendency was found for temperature effect at constant moisture content. *SEI* followed the same trend as *VEI*. The amylose content, which is taken into account by melt storage modulus, had positive effect on *VEI*. These results illustrated the direct effect of shear viscosity, melt storage modulus, moisture content and temperature on expansion, as shown in the concept map (Fig. 1).

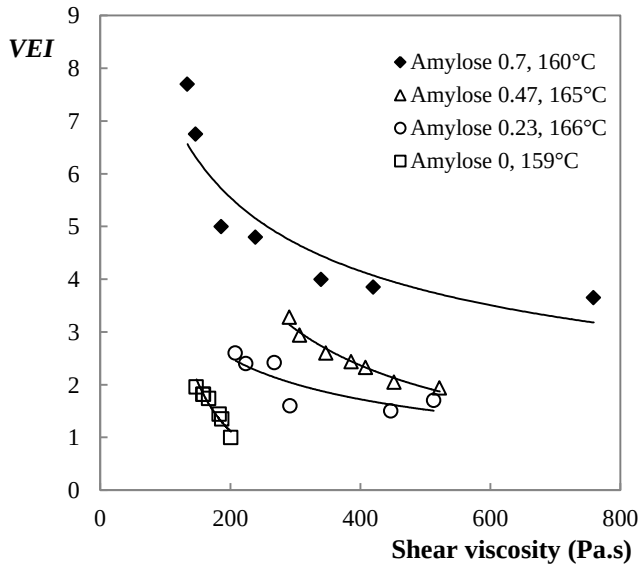

Figure 4. Variation of measured volumetric expansion index (*VEI*) with melt shear viscosity for different amylose contents (*MC* = 0.245 (mass fraction on total wet basis), T_p = 160-165 °C, 200 < *SME* < 250 kWh/t).

As this trend was observed for most extrusion conditions, and following the concept map (Fig. 1),

we proposed to model expansion indices with power type functions:

$$VEI = \alpha_v \left(\frac{\eta}{\eta_0} \right)^{n_V} \quad (11)$$

$$SEI = \alpha_s \left(\frac{\eta}{\eta_0} \right)^{n_S} \quad (12)$$

and the effect of the processing variables on both α_i and n_i by:

$$\alpha_i = b_0 (MC / MC_0)^{b_1} (T_p / T_0)^{b_2} (SME / SME_0)^{b_3} (E' / E'_0)^{b_4} (h / h_d)^{b_5} \quad (13)$$

$$n_i = b_6 (MC / MC_0)^{b_7} (T_p / T_0)^{b_8} (SME / SME_0)^{b_9} (E' / E'_0)^{b_{10}} (h / h_d)^{b_{11}} \quad (14)$$

The processing variables with subscript 0 were used with the aim to obtain dimensionless values. h_d is the height of slit die (or the height of the measuring channel of Rheopac); h is the orifice opening of the entrance of the measuring channel. E' is the storage modulus at glass transition temperature. The variation of E' with amylose and moisture content can be estimated from literature [1, 24]. The same reference for processing variables was used for modeling *VEI* and *SEI*: MC_0 = 0.205, T_0 = 160°C, SME_0 = 200 kWh/t, η_0 = 1000 Pa.s, E'_0 = 485 MPa.

12 parameters may appear as a heavy set for the model, but it was supported by the large number of experimental data (about 400) leading to a large *dof* value and a low *F* value, as shown from the results of statistical analysis at significance level of 0.05 (Tables 3 and 4). They allowed to consider not only the R^2 but also the adjusted R^2, which reflected the robustness of the model, whereas the *t* value of Student Test, computed for each parameter expressed its significance at 0.05.

The term h/h_d may represent the deformation history in the slit die. If this term was neglected, the model fitted poorly the experimental data, R^2 = 0.65 and 0.47, for *VEI* and *SEI*, respectively. Alvarez-Martinez et al. [18] incorporated the term of total strain in the die into their general expansion model, and suggested it characterized the effect of alignment of amylose and amylopectin chains and elastic energy storage of the melt.

Della Valle et al. [15] pointed out the important role of T_g which evolves in function of moisture content (evaporation) during expansion. They supposed that the product structure is fixed during expansion at a temperature 30°C higher than T_g. We did not consider the effect of (T_p - T_g) at the die exit in our

Statistic result			$F_{crit.}$
F value for Levene Test		1.543	3.866
F value for *F*-Test		251.1	1.815
R^2		0.8833	
R^2 adj		0.8798	
RMSE		0.2531	
Model parameters		Standard error	$t_{calc.}$*
b_0	9.87	0.160	17.7
b_1	-4.71	0.162	29.1
b_2	-1.71	0.209	8.2
b_3	n.s.		
b_4	0.37	0.017	22.4
b_5	0.21	0.025	8.2
b_6	-0.15	0.03	5
b_7	1.23	0.363	3.4
b_8	-1.92	0.475	4
b_9	-1.48	0.236	6.3
b_{10}	n.s.		
b_{11}	-0.4	0.062	6.4

Significance level 0.05
*t_{crit} = 1.967
n.s. = not significant

Table 3. Results of statistical analysis for *VEI* model

Statistic result			$F_{crit.}$
F value for Levene Test		1.052	3.866
F value for *F*-Test		113.2	1.815
R^2		0.7733	
R^2 adj		0.7665	
RMSE		0.2844	
Model parameters		Standard error	$t_{calc.}$*
b_0	5.09	0.203	14.33
b_1	-4.6	0.206	22.32
b_2	-2.74	0.213	12.87
b_3	-0.25	0.052	4.8
b_4	n.s.		
b_5	0.46	0.028	16.28
b_6	-0.076	0.036	2.13
b_7	4.92	1.369	3.59
b_8	n.s.		
b_9	n.s.		
b_{10}	0.9	0.302	2.98
b_{11}	-0.88	0.175	5.04

Significance level 0.05
*t_{crit} = 1.967
n.s. = not significant

Table 4. Results of statistical analysis for *SEI* model

models because the difference in T_g between the four starches was small. The T_g of the four starch blends at a fixed moisture content can be calculated using Couchman-Karasz equation for a ternary system (amylose-amylopectin-water), considering at a moisture content of 0.2 (mass fraction on total wet basis), for maize starch with amylose content of 0.7, 0.47, 0.23 and 0.0, that the values of T_g are 32, 30, 29 and 27 °C, respectively [26].

The predicted effect of amylose content on *VEI* in function of shear viscosity is shown in Fig. 5. A fair agreement was obtained between predicted and published experimental results. For the same values of moisture content and temperature, different values of *VEI* were found, at constant shear viscosity, for different amylose contents. Fig. 5 also shows that the influence of the change of amylose content could be taken into account by the change of storage modulus ($E'(T_g)$), and thus of the elongational viscosity, as one of model variables. Using approximate $E'(T_g)$, the models (Eqs. (11-14)) were able to predict correctly the behavior of macrostructure in function of amylose content. At the same shear viscosity, the predicted *VEI* increased with amylose content (with elongational viscosity) for moisture content 0.245 and T_p in the range 159-165°C.

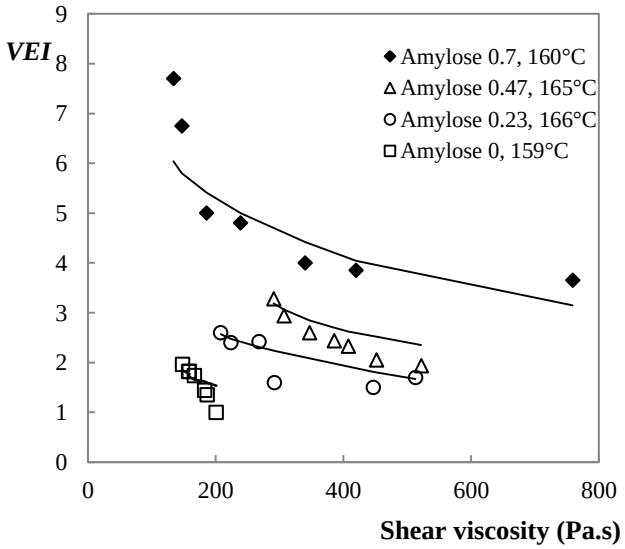

Figure 5. Comparison between experiment and simulation. Effect of amylose content on *VEI* at $150 < SME < 250$ kWh.t^{-1}. Amylose content is taken into account by the melt storage modulus. Symbols represent measured value. Lines represent predicted values using the model.

3.4 Relation between macrostructure and cellular structure

We established the mapping of anisotropy and corresponding cellular structure (Fig. 6) using literature data [1]. The anisotropy was presented by the variation of longitudinal expansion index *LEI* with square root of radial expansion index *SEI*. There is a general trend of *LEI* to be correlated negatively with *SEI*, which is marked by iso-density curves. *LEI* increases with amylose content whereas *SEI* increases with amylopectin content.

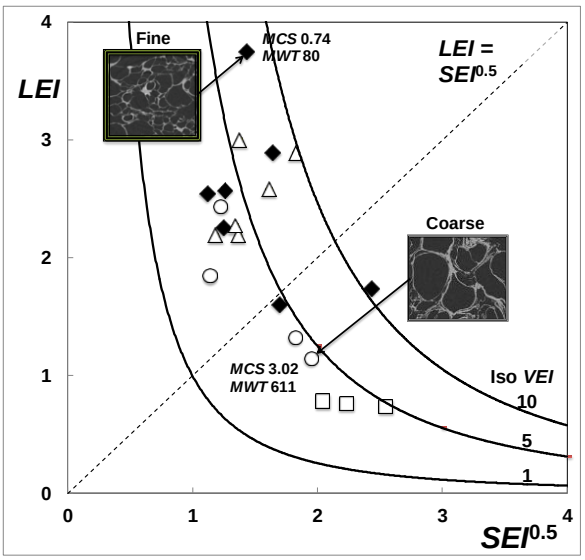

Figure 6. Mapping of anisotropy and cellular structure. Amylose content: ♦ 0.7 ; Δ 0.47; ○ 0.25; □ 0

From Fig. 6, the higher amylose content, the higher was anisotropy factor obtained with favored longitudinal expansion ($LEI >> SEI^{0.5}$). On the other hand, radial expansion was more favored at higher amylopectin content ($LEI << SEI^{0.5}$). Extruded foams with favored longitudinal expansion were characterized by finer cells and thinner cell wall than those for which radial expansion was favored, characterized by coarser cells and thicker cell wall.

The higher elongational viscosity limits bubble coalescence (Fig. 1) because of higher melt resistance to stretching forces during bubble growth, and has a positive effect on expansion. Conversely, the shear viscosity of starch has a negative effect on bubble growth (Fig. 1). Since both viscosities increase with amylose content, their effect on *VEI* could be assessed by the balance between shear and elongational viscosities, i.e. the Trouton number.

According to Alvarez-Martinez et al. [18], the molecular structure could play a role in controlling anisotropy of expansion. The aligned straight chain of amylose would be more difficult to pull apart, thus to swell at the die exit, than the aligned amylopectin that contains many side-branches, so the *SEI* would be lower for starch with important amylose content. The high *L*/*D* ratio of the die also strengthens this effect.

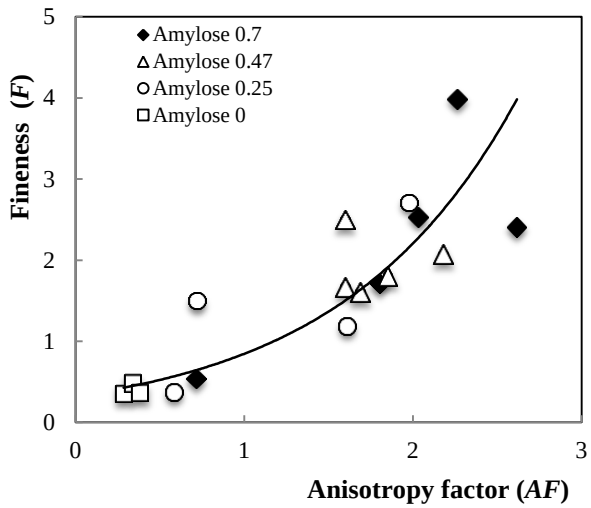

Figure 7. Scaling down from macroscopic structure (anisotropy factor) to microscopic structure (cell fineness)

Finally, there was a good fit (R^2 = 0.82) between cell fineness (*F*) and anisotropy factor (*AF*) computed from experimental data of *MCS*, *MWT*, *VEI* and *SEI* [1] (Fig. 7):

$$F = 0.32 \exp(0.96\, AF) \quad (15)$$

This result showed that the anisotropy *AF* computed from *VEI* and *SEI* models can be used to predict cellular fineness quantitatively using Eq. (15).

4. Conclusion

By reasoning qualitatively from literature and expertise, we have built a concept map which provides a good understanding of the effect of material properties and processing variables on vapor expansion phenomena during extrusion.

Consequently, power law models of bulk expansion indices have been determined with good fit and satisfactory prediction capacity, involving rheological properties, elongational viscosity being represented by melt storage moduli *E*' (at $T > T_g$). Die geometry, likely reflecting the melt deformation history in the die, cannot be neglected. Scale down form macroscopic expansion indices to cellular structural features could be achieved since the cell fineness was modeled as a function of computed anisotropy factor.

These models will now be validated with experimental data from literature, reflecting different operating conditions and materials, for example extrusion of whole wheat flour [2, 27], for which rheological properties are available. This approach can also involve the glass transition temperature T_g which reflects the effect on expansion of more complex formulation (addition of sugar, salt, fiber, etc. in the feed).

Then the models could be integrated into the interface of Ludovic® in order to predict macro- and cellular structures of starchy foams.

References

[1] Babin, P., Della Valle, G., Dendievel, R., Lourdin, D., Salvo, L. X-ray tomography study of the cellular structure of extruded starches and its relations with expansion phenomenon and foam mechanical properties. *Carbohydr. Polym.*, 68, 329-340 (2007).

[2] Robin, F., Engmann, J., Pineau, N., Chanvrier, H., Bovet, N., Della Valle, G. Extrusion, structure and mechanical properties of complex starchy foams. *J. Food Eng.*, 98, 19-27 (2010).

[3] Amon, M., Denson, C.D. A study of the dynamics of foam growth: Analysis of the growth of closely spaced spherical bubbles. *Polym. Eng. Sci.*, 24, 1026-1034 (1984).

[4] Arefmanesh, A., Advani, S.G., Michaelides, E.E. An accurate numerical solution for mass diffusion-induced bubble growth in viscous liquids containing limited dissolved gas. *Int. J. Heat Mass Tran.*, 35, 1711-1722 (1992).

[5] Fan, J., Mitchell, J.R., Blanshard, J.M.V. A computer simulation of the dynamics of bubble growth and shrinkage during extrudate expansion. *J. Food Eng.*, 23, 337-356 (1994).

[6] Arefmanesh, A., Advani, S.G. Nonisothermal bubble growth in polymeric foams. *Polym. Eng. Sci.*, 35, 252-260 (1995).

[7] Schwartzberg, H.G., Wu, J.P.C., Nussinovitch, A., Mugerwa, J. Modelling deformation and flow during vapor-induced puffing. *J. Food Eng.*, 25, 329-372 (1995).

[8] Ramesh, N.S., Malwitz, N. A non-isothermal model to study the influence of blowing agent concentration on polymer viscosity and gas diffusivity in thermoplastic foam extrusion. *J. Cell. Plast.*, 35, 199-209 (1999).

[9] Shimoda, M., Tsujimura, I., Tanigaki, M., Ohshima, M. Polymeric foaming simulation for extrusion processes. *J. Cell. Plast.*, 37, 517-536 (2001).

[10] Alavi, S.H., Rizvi, S.S.H., Harriott, P. Process dynamics of starch-based microcellular foams produced by supercritical fluid extrusion. II: Numerical simulation and experimental evaluation. *Food Res. Int.*, 36, 309-319 (2003).

[11] Wang, L., Ganjyal, G., Jones, D.D., Weller, C.L., Hanna, M.A. Modeling of bubble growth dynamics and nonisothermal expansion in starch-based foams during extrusion. *Adv. Polym. Tech.*, 24, 29-45 (2005).

[12] Pai, D.A., Blake, O.A., Hamaker, B.R., Campanella, O.H. Importance of extensional rheological properties on fiber-enriched corn extrudates. *J. Cereal Sci.*, 50, 227-234 (2009).

[13] Vergnes, B., Della Valle, G., Delamare, L. A global computer software for polymer flows in corotating twin screw extruders, *Polym. Eng. Sci*., 38, 1781-1792 (1998).

[14] Della Valle, G., Colonna, P., Patria, A. Influence of amylose content on the viscous behavior of low hydrated molten starches. *J. Rheol*., 40, 347-362 (1996).

[15] Della Valle, G., Vergnes, B., Colonna, P., Patria, A. Relations between rheological properties of molten starches and their expansion behaviour in extrusion. *J. Food Eng*., 31, 277-295 (1997).

[16] Vergnes, B., Della Valle, G., Tayeb, J. A specific slit die rheometer for extruded starchy products. Design, validation and application to maize starch, *Rheol. Acta*, 32, 465-476 (1993).

[17] Della Valle, G., Kozlowski, A., Colonna, P., Tayeb, J. Starch transformation estimated by the energy balance on a twin-screw extruder. *Lebensm. Wiss. Technol*., 22, 279-286 (1989).

[18] Alvarez-Martinez, A., Kondury, K.P., Harper, J.M. A general model for expansion of extruded products. *J. Food Sci*., 53, 609-615 (1988).

[19] Arhaliass, A., Bouvier, J. M., Legrand, J. Melt growth and shrinkage at the exit of the die in the extrusion-cooking process. *J. Food Eng*., 60, 185–192 (2003).

[20] Berzin, F., Tara, A., Tighzert, L., Vergnes, B. Importance of coupling between specific energy and viscosity in the modeling of twin screw extrusion of starchy products. *Polym. Eng. Sci*., 50, 1758-1766 (2010).

[21] Comuzzi, C., Polese, P., Melchior, A., Portanova, R., Tolazzi, M. SOLVERSTAT: a new utility for multi-purpose analysis. An application to the investigation of dioxygenated Co(II) complex formation in dimethyl-sulfoxide solution. *Talanta*, 59, 67-80 (2003).

[22] Della Valle, G., Vergnes, B., Lourdin, D. Viscous properties of thermoplastic starches from different botanical origin. *Intern. Polym. Proc*., 22, 471-479 (2007).

[23] Brent, J. J. L., Mulvaney, S. J., Cohen, C., Bartsch, J. A. Viscoelastic properties of extruded cereal melts. *J. Cereal Sci*., 26, 313–328 (1997).

[24] Ditudompo , S., Takhar, P.S., Ganjyal, G.M., Hanna, M.A. The effect of temperature and moisture on the mechanical properties of extruded corn starch. *J. Text. Stud*., 44, 225-237 (2013).

[25] Robin, F., Dattinger, S., Boire, A., Forny, L., Horvat, M., Schuchmann, H.P., Palzer, S. Elastic properties of extruded starchy melts containing wheat bran using on-line rheology and dynamic mechanical thermal analysis. *J. Food Eng*., 109, 414-423 (2012).

[26] Bizot, H., Le Bail, P., Leroux, B., Davy, J., Roger, P., Buleon, A. Calorimetric evaluation of the glass transition in hydrated, linear and branched polyanhydroglucose compounds. *Carbohydr. Polym.*, 32, 33-50 (1997).

[27] Robin, F., Dubois, C., Pineau, N., Labat, E., Théoduloz, C., Curti, D. Process, structure and texture of extruded whole wheat. *J. Cereal Sci*., 56, 358-366 (2012).

[Abridged French version]

Modèle phénoménologique de l'expansion d'amidons en extrusion

Dans le procédé de cuisson-extrusion des produits amylacés, la matière fondue est forcée à travers une filière. La détente instantanée à la sortie de la filière entraine l'auto-vaporisation de l'eau, donc la formation des bulles, accompagnée par une baisse de la température du produit, de la teneur en eau, et donc une augmentation de la température de la transition vitreuse T_g. C'est un phénomène complexe qui englobe la dynamique de nucléation, de croissance, de coalescence et de rupture des bulles dans une matrice viscoélastique, puis la solidification, voire l'effondrement à proximité de T_g. A l'heure actuelle, aucun-modèle déterministe n'est disponible pour décrire ces phénomènes conjointement. En outre, un modèle déterministe serait trop complexe et ne pourrait être couplé avec le modèle mécanistique du logiciel de simulation d'extrusion bi-vis (Ludovic®), afin de prédire directement la structure cellulaire des mousses amylacées.

L'objectif de ce travail est d'élaborer un modèle phénoménologique d'expansion afin de pouvoir le coupler avec Ludovic®. A partir de résultats expérimentaux de la bibliographie qui couvrent un large domaine de conditions thermomécaniques (environ 400 points expérimentaux), une carte conceptuelle qui décrit des relations d'influence entre les variables d'entrée et de sortie du modèle d'expansion a été construite. Elle prend en compte les phénomènes de nucléation, croissance de bulles, coalescence, rupture et fixation. Les variables d'entrée, telles que la température T, l'énergie mécanique spécifique SME et la viscosité en cisaillement η à la sortie de la filière, peuvent être calculées par Ludovic®. Les autres sont la teneur en eau MC, la géométrie de la filière h/h_d et le module de stockage E'(à $T > T_g$). Cette dernière propriété représente la viscosité élongationelle des amidons pour une teneur en amylose variable (0-70%). Les variables de sortie

sont la macrostructure et la structure cellulaire des mousses solides. La macrostructure est décrite par les indices d'expansion et l'anisotropie. La finesse de la cellule *F*, calculée à partir de la taille moyenne des cellules *MCS* et de l'épaisseur moyenne de la paroi cellulaire *MWT*, définit la structure cellulaire. Par la suite, une expression mathématique générale du modèle est proposée pour *VEI* et *SEI*, les indices d'expansion volumétrique et radiale, respectivement: VEI et $SEI = \alpha\,(\eta\,/\,\eta_0)^n$ avec α et n dépendant de *T*, *MC*, *SME*, h/h_d et *E'*. A partir des valeurs connues de *VEI* et *SEI*, nous avons pu prédire l'anisotropie d'expansion (*AF*) par la relation $AF = VEI\,/\,SEI^{3/2}$. Un bon accord entre les résultats de simulation et ceux expérimentaux est obtenu. En outre, nous avons montré que la finesse de cellule *F* peut être modélisée en fonction de l'anisotropie *AF*.